

We are IntechOpen, the world's leading publisher of Open Access books Built by scientists, for scientists

4,800

Open access books available

122,000

International authors and editors

135M

Downloads

Our authors are among the

154

Countries delivered to

TOP 1%

most cited scientists

12.2%

Contributors from top 500 universities



WEB OF SCIENCE™

Selection of our books indexed in the Book Citation Index
in Web of Science™ Core Collection (BKCI)

Interested in publishing with us?
Contact book.department@intechopen.com

Numbers displayed above are based on latest data collected.
For more information visit www.intechopen.com



XAFS and IR Studies on Luminescent Silver Zeolites

Takafumi Miyanaga, Yushi Suzuki and Sho Narita

Additional information is available at the end of the chapter

<http://dx.doi.org/10.5772/63904>

Abstract

In this chapter, studies of structures and optical properties of Ag-zeolite A by means of X-ray absorption fine structure (XAFS) and infrared (IR) spectra are presented. XAFS is a powerful tool to study the local structure of Ag nanoclusters in the zeolite cavity and IR spectra are quite sensitive to the change in zeolite lattice affected by the production of Ag clusters. First, we focus on the creation of Ag clusters in zeolite A by heat treatment under atmosphere and vacuum. Second, we discuss the mechanism of photoluminescence for Ag-zeolite composite. It is widely believed that the emitting point is Ag clusters in the Ag zeolite; on the other hand, our recent result is contradicted that Ag clusters are broken down in the strongly emitting species.

Keywords: silver zeolite A, Ag cluster, photoluminescence, XAFS, IR spectroscopy

1. Introduction

Ag zeolites are versatile family of functional materials: application to catalysis, anti-bacterial materials, information storage, pressure, and chemical sensors. In the field of nanoscaled science, the metal nanoparticles and nanoclusters are quite quite attractive. Using the zeolite cavity, nanoparticles and clusters are produced simply and the particle size is easily controlled [1–4]. However, the structural effect of zeolite lattice is not so well known that the structure and properties of nanoparticles and clusters are quite complicated.

Optical properties of small metal clusters are intriguing research topics today. Luminescence from the metal clusters is an attractive subject and especially silver and gold clusters show brilliant emission. This luminescent behavior can be expected by industry market without rare-earth metals. Recently, the characterization of photo luminescence from heat-treated Ag zeolites is extensively investigated [5–7]. So far, the luminescent species are widely believed

to be Ag clusters or oligomers produced in the cavity of zeolite. However, there are still ambiguous points and hot discussions in the field of luminescent Ag zeolite.

X-ray absorption fine structure (XAFS) has characteristic features that elemental selectively analyzed with local structure for such complex systems. In the case of Ag zeolites, the local and electronic structure around Ag atoms has been extensively investigated [8–11]. On the other hand, infrared (IR) spectra are sensitive to molecular atomic vibration of zeolite lattice. In this chapter, we present the introduction of XAFS and IR spectroscopy first and then discuss (1) the creation of Ag clusters in the cavity of zeolite A and (2) the mechanism of photoluminescence (PL) of Ag-zeolite composites by the use of XAFS and IR spectra [12].

2. X-ray absorption fine structure and infrared spectra

In this section, we show the outline of the tools for the investigation of the structure and electronic states of Ag zeolites: XAFS and IR.

2.1. XAFS spectroscopy

We present the basic description of XAFS technique theoretically and experimentally. XAFS is the fine structure observed on X-ray absorption coefficient spectra near the absorption edge of a particular element. When monochromatic X-rays are irradiated on a sample, the intensity of the transmitted X-ray, I_t , depends on the photon energy E and sample thickness d (Figure 1). According to the Beer-Lambert law, I_t is expressed as

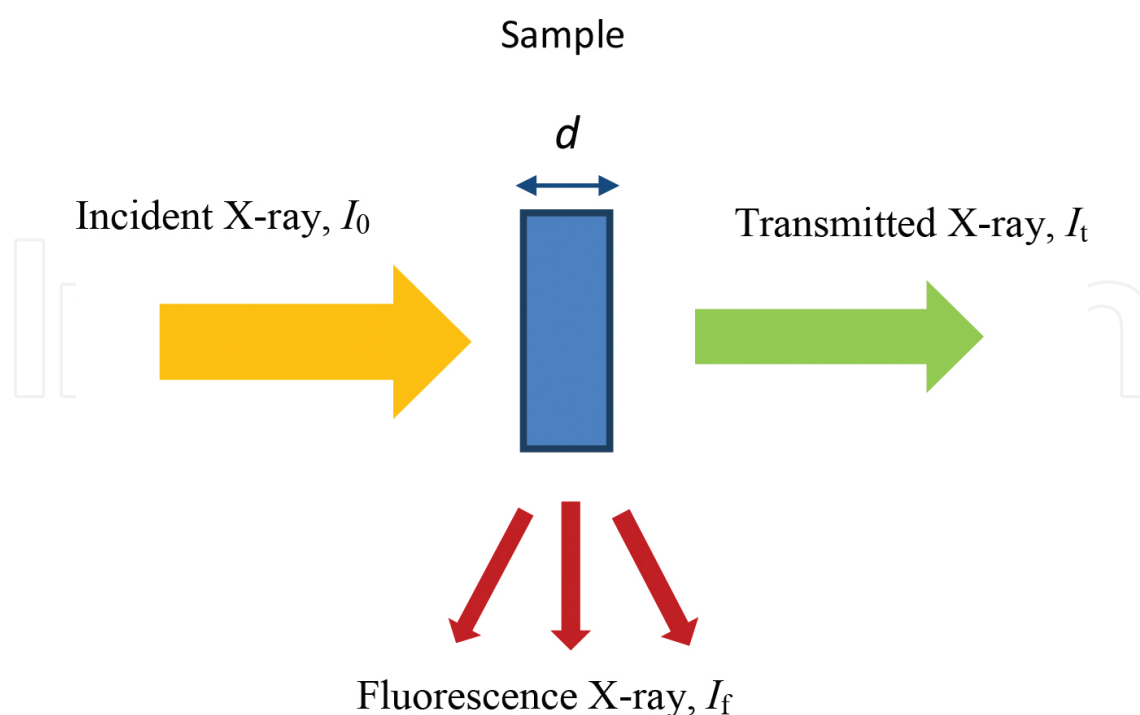


Figure 1. Schematic representation of transmission and fluorescence mode for X-ray absorption.

$$I_t = I_0 e^{-\mu(E)d} \quad (1)$$

Here, I_0 is the intensity of the incident X-ray and $\mu(E)$ is the energy-dependent X-ray absorption coefficient. Since $\mu(E)$ is approximately proportional to $a Z^4/m E^3$ where a , Z , and m are, respectively, the density of the sample, atomic number, and electron mass, the $\mu(E)$ decreases monotonically as a function of X-ray energy. When the X-ray energy has an exciting energy of a core electron, the core electron ejects to continuum state. In that time, the X-ray photon is annihilated in order to create a photoelectron and a core hole. As the result, $\mu(E)$ shows stepwise increase at the energy of core electron excitation (absorption edge). The core hole recombines with an electron from the higher energy level; X-ray fluorescence or the creation of an Auger electron is emitted.

In the X-ray energy region generally 60–1000 eV from the absorption edge, the equation of the absorption coefficient can be simplified under the following approximations as the Muffin-tin approximation for the atomic potential, the one-electron process in the absorption, the dipole approximation for the interaction between X-ray and matter, the plane-wave approximation for the propagating photoelectron, and the single scattering process considered in the scattering process. The X-ray absorption profile in this high-energy region is called Extended XAFS (EXAFS), where function $\chi(k)$ is expressed as

$$\chi(k) = \sum_j \frac{N_j S_0^2}{k r_j^2} \left| f_j(k, \pi) \right| e^{\left(-2 \left(\sigma_j^2 k^2 + r_j / \lambda(k) \right) \right)} \sin \left(2k r_j + 2\delta_i(k) + \phi_j(k) \right), \quad (2)$$

where r_j , N_j , and σ_j are the interatomic distance between X-ray absorbing atom i and electron scattering atom j , the coordination number of scattering atom j , and the root-mean-square relative displacement (or Debye-Waller factor) of the atomic pair ij , respectively. These unknown structural parameters can be determined by the use of the nonlinear least-square-fitting (the so-called curve-fitting) method; for example, XANADU [13] code and Athena & Artemis code [14]. The phase shift of the photoelectron $\phi_j(k)$, the electron backscattering amplitude $f_j(k)$, and the electron mean free path “lambda(symbol)” (k) in the medium are generally calculated from theoretically, for example, FEFF code [15].

The X-ray absorption coefficient can be determined from the ratio of intensities for the incident and transmitted X-ray as transmission mode, X-ray fluorescence as fluorescence mode, or Auger electrons as electron yield mode.

The intensity of incident and transmitted X-ray is measured using ionization chambers filled by inert gas. For transmission measurements, appropriate concentration is important for sample preparation. And then, the samples are required to be homogeneous and to have a constant thickness without pinholes. the samples are prepared by grinding and mixed with a suitable binder such as BN as transparent to X-rays in general.

We apply the transmission mode for the XAFS measurement of Ag zeolites. The Ag *K*-edge (25 keV) XAFS were measured at NW10A on PF-AR at KEK using Si(311) monochromator. We use in situ sample chamber shown in **Figure 2**, in which temperature can be controlled from LN₂ temperature to 773 K and the introduction of the various gasses is available.

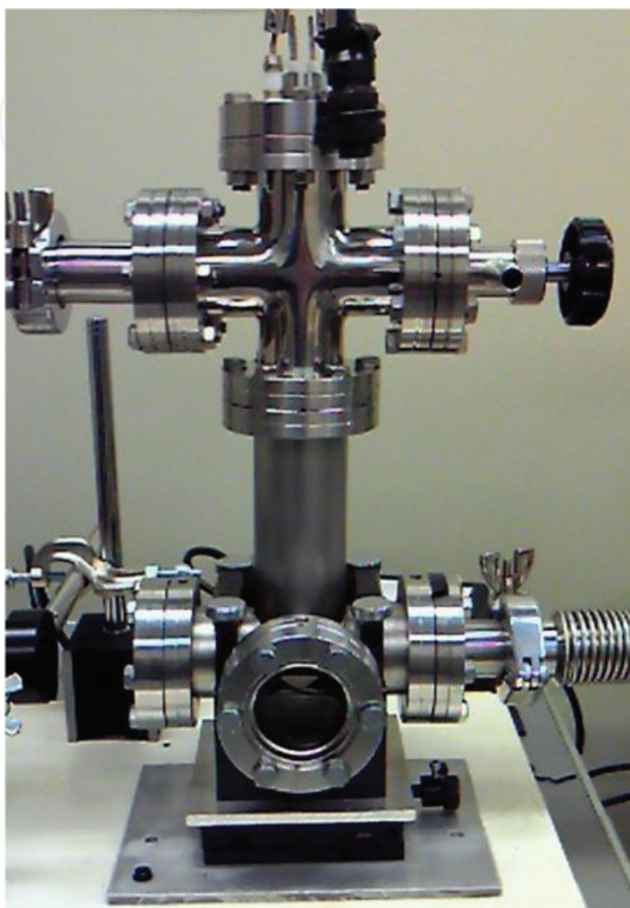


Figure 2. In situ cell chamber for the measurement of Ag *K*-edge XAFS and IR spectra for Ag zeolites.

2.2. IR spectroscopy: basics and measurements

In this subsection, the method of infrared spectra is described. Vibrational spectroscopy has gained wide recognition for its ability to determine the chemical nature of materials. Three techniques have emerged to be most useful, namely Infrared Spectroscopy (IR), Electron Energy Loss Spectroscopy (EELS), and Raman Spectroscopy. Infrared spectroscopy has achieved high sensitivity at high resolution. Furthermore, this technique has proven to be most valuable due to its ability to work at ambient pressure from ultra-high vacuum (UHV) to atmosphere. EELS is restricted to UHV pressures and homogeneous (i.e., orders) surface. Since in the measurement of zeolite the coexistence gas is important, EELS is not suitable. Raman spectroscopy commonly used visible light as the excitation light, the energy is close to the PL excitation energy of Ag zeolite, and it would give a perturbation to the system. In addition, Raman spectroscopy has the disadvantage of sensitivity and is not suitable for the zeolite.

In XAFS, high-energy X-rays are used as probes, whereas low-energy infrared light is used in the IR as a probe. In the measurement of the Ag zeolite, XAFS detects the local structure around Ag atom but IR does that of the framework of zeolite. Thus, on measuring Ag zeolite, XAFS and IR can be said to be best partner for obtaining the complementary structural information.

The IR light absorption spectra were obtained at normal incidence of radiation. The infrared measurements were performed on an ABB BOMEM MB-100 spectrometer equipped with a DTGS detector at 4 cm^{-1} resolution with 128 interferometric scans. Zeolite powder was deposited on the Si wafer, and then an excessive specimen was blown off with a hand blower. A small quantity of zeolite was stuck electrostatically. The Si was installed with a sample into the in situ chamber cell as shown in **Figure 2**. The principle of signal collection is similar to the XAFS, as described in Eq. (1).

3. Sample preparation

The fully Ag^+ -exchanged zeolite A was prepared by immersing the hydrated 12Na-A in 0.1-M AgNO_3 solution for 24 h at 25°C . The solution was stirred every 1 h. After careful filtration, the Ag-zeolite-A powder was dried under air at room temperature (RT) in the dark space.

We apply two kinds of methods for producing Ag clusters in the cavity as follows:

- (a) Ag-zeolite A was heated at $300\text{--}500^\circ\text{C}$ in vacuum to produce the Ag clusters [11]. After maintaining at high temperature for 24 h, it was cooled to room temperature, and then various gases, air, O_2 , N_2 , H_2O , and their mixtures, are introduced.
- (b) Ag-zeolite A was heated at $300\text{--}500^\circ\text{C}$ under atmosphere and maintained at the same temperature for 24 h. After that, it is cooled to room temperature under atmosphere (with air).

For both processes, the samples were kept for long time (about 24 h) after cooling to room temperature.

4. Creation of Ag clusters in zeolite A cavity

In this section, we discuss the creation of Ag clusters in the zeolite cavity of zeolite A with heat treatment under atmosphere or vacuum studied by using XAFS.

Figure 3 shows the typical example of Fourier transform (FT) of the Ag K-edge EXAFS spectra for the hydrated Ag-zeolite A measured at RT atmosphere and after heating at 300°C under vacuum. We can find two main peaks in FT: the first peak at around 2.2 \AA and the second one at around 3.0 \AA . The first peak is higher than the second one for the hydrated Ag-zeolite A, while the second peak is higher than the first one for the dehydrated Ag-zeolite A under vacuum. This phenomenon indicates that the Ag clusters are produced by heating at least 300°C under vacuum.

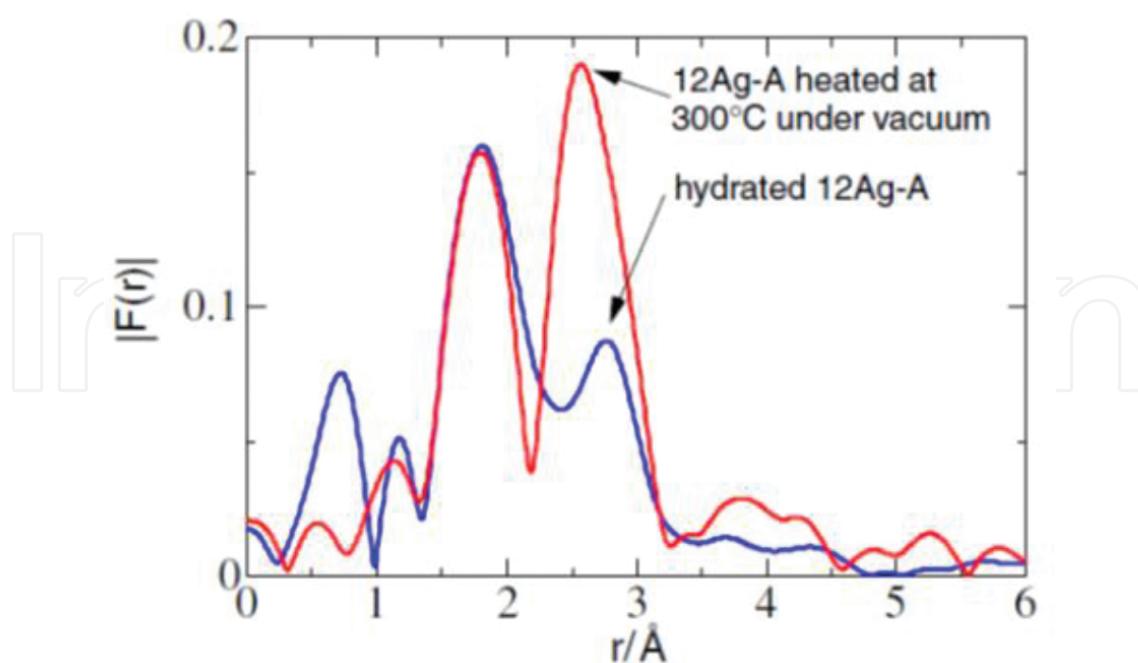


Figure 3. Fourier transforms (FT) of the Ag K-edge EXAFS spectra for the hydrated Ag-zeolite A measured at RT atmosphere and measured at RT after heating at 300 °C under vacuum [11].

Figure 4 shows $k^2\chi(k)$ spectra measured by quick EXAFS mode in the process of heating to 500°C atmosphere. Each spectrum was measured about 50 s and the corresponding sample temperatures are presented. The large structural change appears at around 150–300°C.

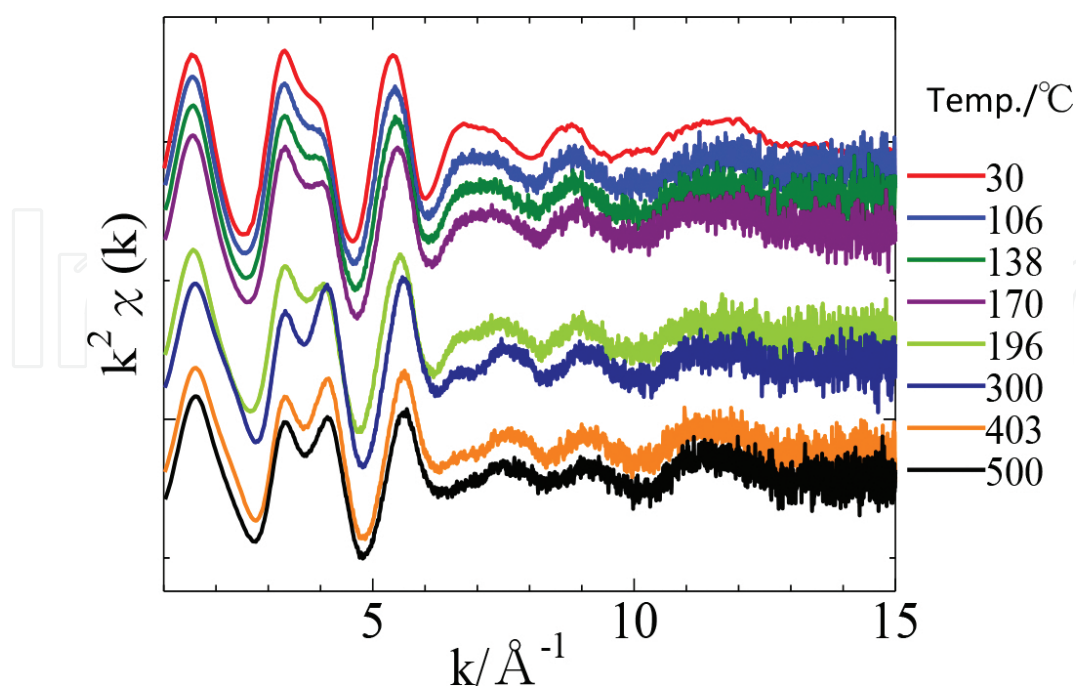


Figure 4. $k^2\chi(k)$ spectra for quick EXAFS measurement in the process of heating to 500°C atmosphere.

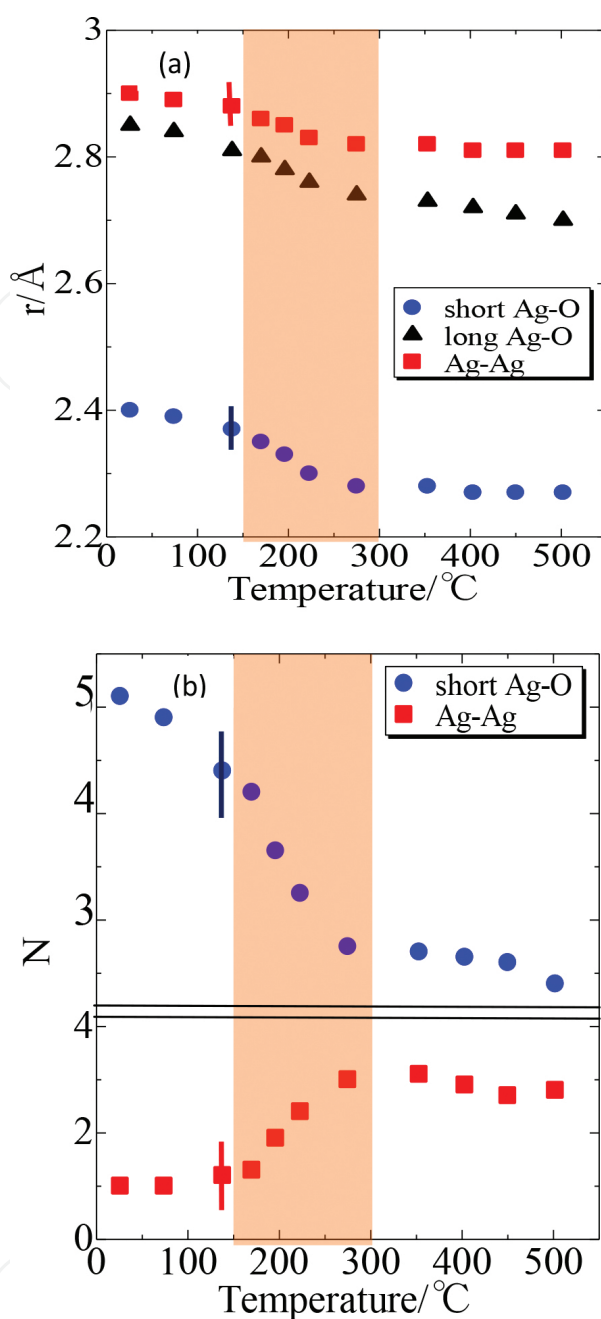


Figure 5. (a) Plots of the interatomic distances, r , and (b) that of the coordination number, N , as a function of measurement temperature.

The structural parameters obtained from the curve-fitting method by the use of Eq. (2) are plotted in **Figure 5(a)** for the interatomic distance, r , and **(b)** for the coordination number, N .

The Ag clustering in zeolite A occurs in the temperature range from 150 to 300°C. In this temperature range, the distance of Ag-O (short) decreases because of dehydration, and that of Ag-Ag also decreases because of less repulsion force between Ag^+ and Ag^0 when Ag^+ reduced by the dehydration. At the same temperature range, the increase of N for Ag-Ag indicates the Ag clustering process.

5. Mechanism of photoluminescence from Ag-zeolite A composites

In this section, we present the observation of PL and discuss the origin of the luminescent point in the Ag zeolite by the use of XAFS and IR. Many researchers believe that the luminescent points are Ag clusters themselves in the zeolite, but our result suggests that the origin of luminescence is the zeolite lattice after affected by the formation of Ag clusters in it.

First, we discuss the result of the PL measurement. **Figure 6** shows the PL curves for various introduction gases after heating of Ag-zeolite A in vacuum. The wavelength of the excitation light is 405 nm. The strongest intensity of PL band around 2.1 eV was observed when the air or the mixture of the $\text{H}_2\text{O} + \text{N}_2$ is introduced. It is suggested that the combination of $\text{H}_2\text{O} + \text{N}_2$ is important for the strong PL band. On the other hand, PL is not observed when the O_2 was introduced. In the present stage, the role of the gases of O_2 , N_2 and H_2O for these phenomena has been unclear.

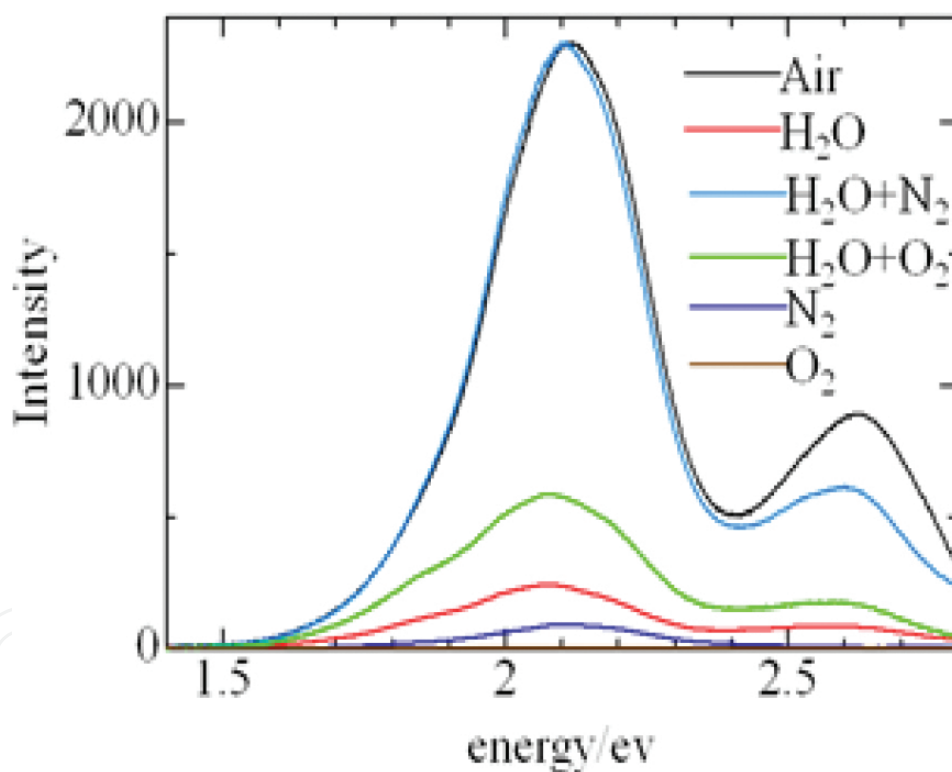


Figure 6. PL curves for various introduction gases after heating of Ag-zeolite A. The wave length of the excitation light is 405 nm [12].

Figure 7 shows the EXAFS $k^2\chi(k)$ spectra for Ag-zeolite A after following gases were introduced: Air, O_2 , N_2 , $\text{H}_2\text{O} + \text{O}_2$, $\text{H}_2\text{O} + \text{N}_2$ with unheated state. The structure around 3.5 \AA^{-1} is returned to unheated state when air or $\text{H}_2\text{O} + \text{N}_2$ was introduced. This reversible change in $k^2\chi(k)$ spectra indicates the breakdown of the Ag clusters. On the other hand, the $k^2\chi(k)$ spectra were not changed when O_2 gas was introduced.

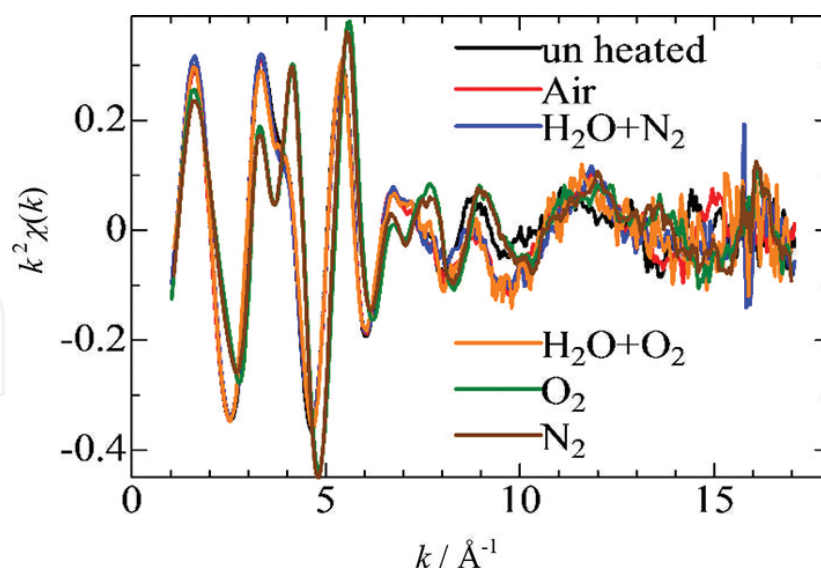


Figure 7. $k^2\chi(k)$ spectra for Ag-type zeolite A after the following gases were introduced: Air, O_2 , N_2 , $H_2O + O_2$, $H_2O + N_2$ with unheated state.

Figure 8 shows the Ag K-edge Fourier transform spectrum for Ag-zeolite A measured at room temperature in atmosphere and that after following gases were introduced: Air, O_2 , N_2 , $H_2O + O_2$, $H_2O + N_2$ with unheated state. The peak at ca 1.7 Å is assigned to the first nearest neighbor (1NN) O1 atom, and the second peak at ca 2.7 Å is to the second nearest neighbor (2NN) O_2 and Ag atom. The three-shell curve-fitting technique was applied and the unknown structural parameters, the atomic distance r and the coordination number N for Ag-O1, Ag-O2, and Ag-Ag, were determined.

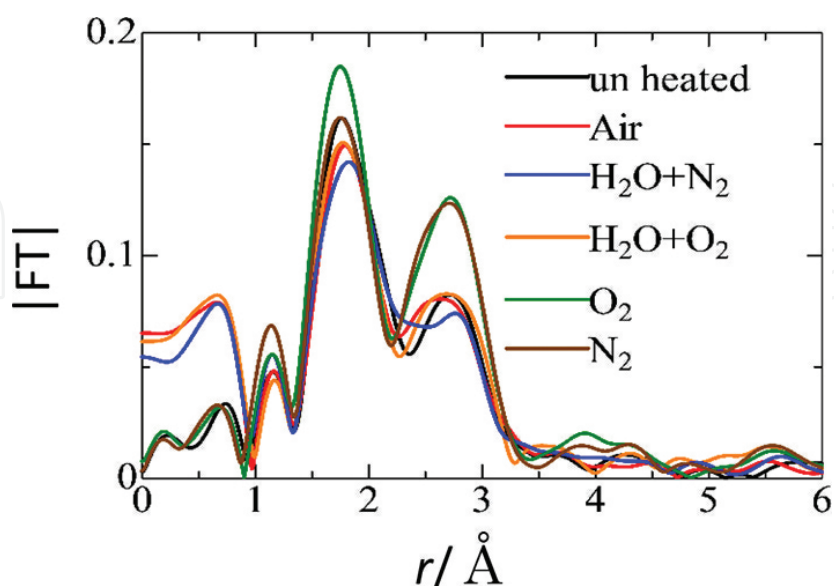


Figure 8. Ag K-edge Fourier transform spectrum for Ag-zeolite A measured at room temperature in atmosphere and that after following gases were introduced: Air, O_2 , N_2 , $H_2O + O_2$, $H_2O + N_2$ with unheated state [12].

Table 1 shows the structural parameters for Ag-zeolite A after the various gases are introduced. We can see in **Figure 6** that after the Air is introduced the strong PL band is observed. The Ag clusters were broken down according to the introduction of the Air. The parameters of r_{Ag} and N_{Ag} are very close to those in atmospheric pressure for the room temperature, which mean no Ag clusters. It takes enough time as 24 hours to breakdown Ag cluster by the introduction of Air. The present PL and XAFS results lead to the fact that the existence of the Ag clusters inhibits the strong PL band. When the O_2 gas is introduced, no PL band is observed. The r_{O1} and r_{Ag} are constant after the O_2 gas is introduced, and the N_{Ag} is still large ($N_{Ag} \sim 2.35$), which indicates that the Ag clusters still exist. We consider the cluster change after the mixed gases of $H_2O + O_2$, and $H_2O + N_2$ are introduced. When $H_2O + O_2$ mixture gases were introduced, weak PL band is detected. On the other hand, strong PL band is observed in the case of $H_2O + N_2$. The N_{Ag-Ag} evaluated from the curve-fitting method shows the breakdown of the Ag clusters similar to the case of the air or both cases $H_2O + O_2$ and $H_2O + N_2$ introduction.

	$r_{O1}(\text{\AA})$	N_{O1}	$r_{O2}(\text{\AA})$	N_{O2}	$r_{Ag}(\text{\AA})$	N_{Ag}
Air	2.38	4.57	2.86	2.96	2.86	1.40
O_2	2.30	4.14	2.85	4.85	2.84	2.35
$H_2O + O_2$	2.39	6.73	2.86	5.19	2.88	0.94
$H_2O + N_2$	2.39	5.75	2.86	4.23	2.87	1.23

Table 1. The structural parameters, r and N after the various gases are introduced [12].

Figure 9 shows the IR result of Ag-zeolite A. The black line shows the IR transmission spectrum of the unheated Ag zeolite. Since the zeolite has a complicated structure and bands are superimposed on the various Si-O and Al-O, it is extremely difficult to distinguish between them. Therefore, assignment of the absorption band around 1000 cm^{-1} region is only represented as $\nu(T-O)$ ($T = \text{Si or Al}$) [16]. Bands appearing at relatively high wavenumber are assigned to the $\nu_{\alpha\sigma}$ mode, and the low wavenumber region is assigned to ν_{σ} mode. Bending mode appears in the lower-energy region, not shown here.

The green line shows that the spectrum of the Ag zeolite was cooled to RT after heating for 24 h at $500\text{ }^{\circ}\text{C}$ in vacuum (measured in a vacuum). As compared to the case of unheated, absorption band has been changed drastically. While individual band assignment is not known as mentioned above, considering the results of XAFS, it is reasonable to assume the change due to the formation of Ag clusters. For cluster formation, it is necessary that Ag^+ ions (at least partially) are reduced to Ag^0 ; also Ag which is to be aggregated away from the site of Ag^+ ion was located. Reduction of ions and changing the position also affect vibration of the framework in each case. (The distance changes between the framework and the Ag atoms and changes in the electrostatic attraction of Ag^+ can perturb the vibration of the T-O. In other words, it can be said that the IR is a sensitive technique to such a change.)

The red line is the spectrum in the case of introducing Air into the zeolite, cooling to RT after the vacuum heating. The spectrum greatly changed again, and is much closer to the spectrum

of the unheated spectrum indicated in the black line. While XAFS for the state that Air intake after heating substantially coincide with that unheated, IR spectra for both state do not match completely each other. Distinct band appeared at 1140 cm^{-1} and the strength of the main band of $1000\text{--}900\text{ cm}^{-1}$ decreased slightly. The cause of this change is not made apparent. However, the state where PL is expressed, that is, in the state where the excitation light is illuminated, the strength of the main band increases and 1140 cm^{-1} band decreases (**Figure 10**). For these reasons, this band change is evident and directly related to PL. As a cause of this change, considering that a change in XAFS is not almost observed, there may be two hypotheses as follows:

- (1) The oxygen deficiency generated in the framework by treatment such as heated in vacuum.
- (2) After Ag clusters collapse, Ag^+ cannot be located in a stable site, “caught” in a metastable site located in the vicinity of stable site. (This metastable site needs a shift of the slight position that cannot be detected by XAFS.)

Since Ag loading into zeolite performed in solution for a sufficient time, Ag^+ ions can be positioned at a stable site. By contrast, disintegration after cluster formation is in atmosphere at room temperature and may not exceed a potential barrier existing between the stable site and the metastable sites.

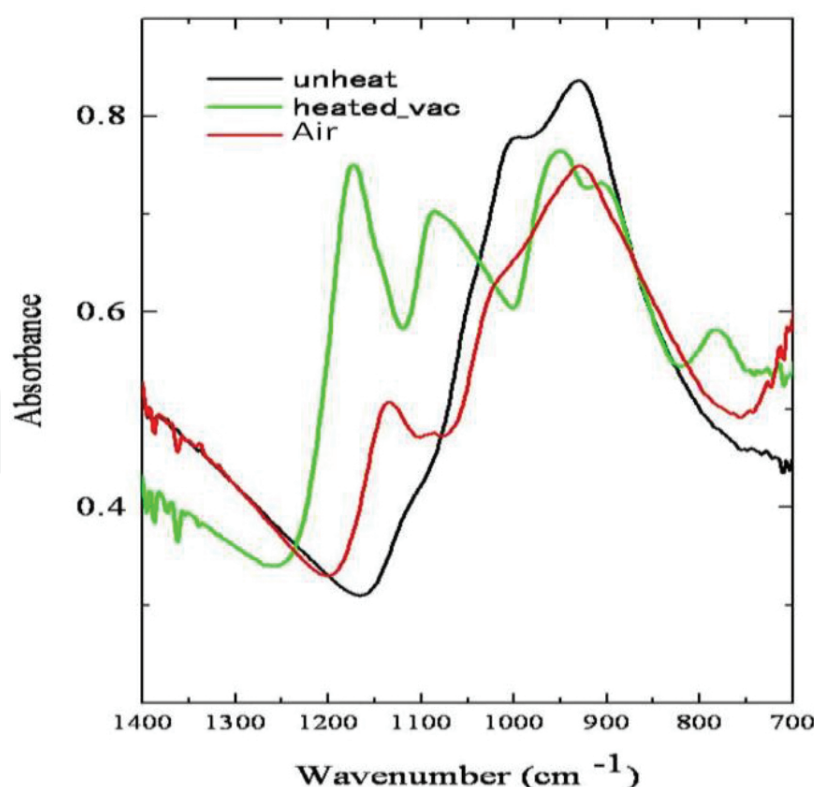


Figure 9. IR spectra for Ag-zeolite; unheated, after heating to $500\text{ }^{\circ}\text{C}$ in vacuum and air introduced after heating.

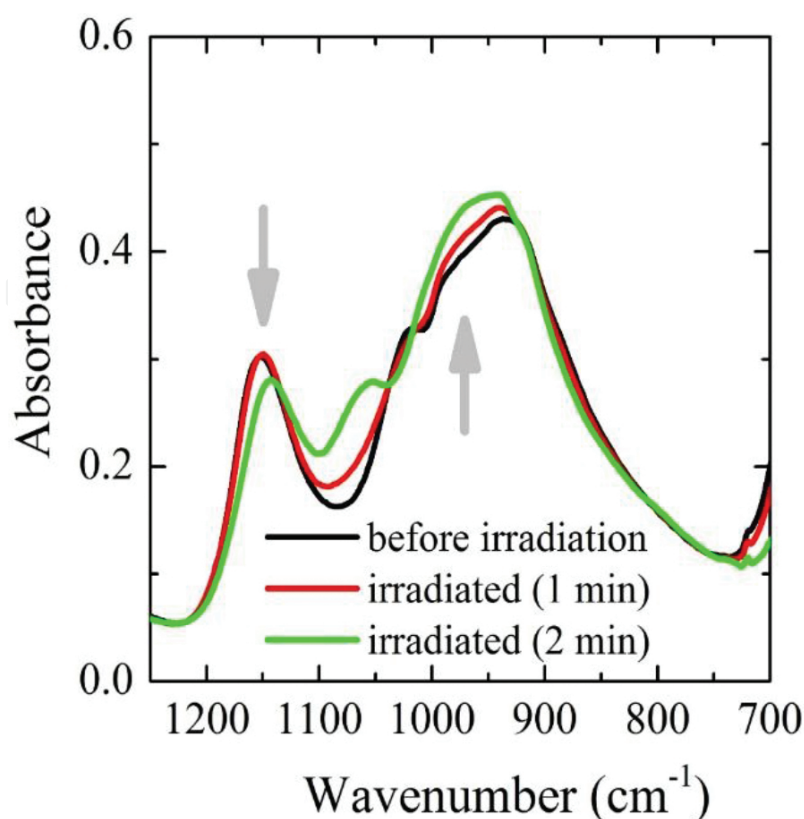


Figure 10. IR spectra for Ag-zeolite; Air introduced after heating (before irradiation), irradiated by excited light (405 nm, 1 min) and irradiated by excited light (405 nm, 2 min).

6. Summary

In this chapter, we discussed the formation of Ag clusters in the Ag-zeolite A cavity and the origin of strong PL after the formation of Ag clusters in zeolite A.

Ag clusters are formed in the cavity of Ag-substituted zeolite A after heat treatment under atmosphere or in vacuum. In the cavity, Ag^+ is reduced by the removal of the water molecule and Ag-O distance decreases. The Ag-Ag distance is also decreased because the repulsion between Ag and Ag is weakened. The coordination number of Ag-Ag is increased to around 2.35 after producing Ag clusters.

On the other hand, strong PL appears at 2.1 eV excited by 405-nm laser with Air or mixed gas of H_2O and N_2 . The present Ag *K*-edge XAFS study indicated the local structure of Ag atoms in chemical species, which shows that the strong PL is almost the same as unheated one and Ag clusters are broken down. The IR spectra in the region of zeolite framework vibration of the species after Ag cluster breakdown are different from the unheated one. This indicates that the framework structure of zeolite changed by the production and breakdown of Ag clusters in the cavity. The effect to zeolite framework has a key for the strong PL.

Acknowledgements

The authors are grateful to Prof. H. Hoshino for the fruitful discussion of XAFS and PL in Ag-zeolite A. The synchrotron radiation experiments were performed at the Photon Factory in KEK.

Author details

Takafumi Miyanaga*, Yushi Suzuki and Sho Narita

*Address all correspondence to: takaf@hirosaki-u.ac.jp

Department of Mathematics and Physics, Hirosaki University, Aomori, Japan

References

- [1] Y. Kim, K. Seff. The octohedral hexasilver molecule. Seven crystal structures of variously vacuum-dehydrated fully Ag⁺-exchanged zeolite A. *J. Am. Chem. Soc.* 1974;100:6989.
- [2] T. Sun, K. Seff. Silver clusters and chemistry in zeolites. *Chem. Rev.* 1994;94(4):857.
- [3] R. Seifert, R. Rytz, G. Calzaferri. Colors of Ag⁺-exchanged zeolite A. *J. Phys. Chem. A.* 2000;104:7473.
- [4] G. Calzaferri, C. Leiggener, S. Glaus, D. Schurch, K. Kuge. The electronic structure of Cu⁺, Ag⁺, and Au⁺ zeolites. *Chem. Soc. Rev.* 2003;32:29.
- [5] G. De Cremer, E. C-Gonzalez, M.B.J. Roefsaers, D.E. De Vos, J. Hofkens, T. Vosch, B. F. Sels. In situ observation of the emission characteristics of zeolite-hosted silver species during heat treatment. *ChemPhysChem.* 2010;11:1627.
- [6] E. C-Gonzalez, M.B.J. Roefsaers, B. Dieu, G. De Cremer, S. Leyre, P. Hanselaer, W. Fyen, B. Sels, J. Hofkens. Determination and optimization of the luminescence external quantum efficiency of silver-cluster zeolite composites. *J. Phys. Chem. C.* 2013;117:6998.
- [7] G. De Cremer, E. C-Gonzalez, M.B.J. Roefsaers, B. Moens, J. Ollevier, M. Van der Auweraer, R. Schooheydt, P.A. Jacobs, F.C. De Schryver, J. Hofkens, D.E. De Vos, D.F. Sels, T. Vosch. Characterization of fluorescence in heat-treated silver-exchanged zeolites. *J. Am. Chem. Soc.* 2009;131:3049.
- [8] T. Miyanaga, H. Hoshino, H. Endo, H. Sakane. EXAFS study of silver clusters in zeolite. *J. Synchrotron Rad.* 1999;6:442.

- [9] T. Miyanaga, H. Hoshino, H. Endo. Local structure of silver clusters in the channels of zeolite 4A. *J. Synchrotron Rad.* 2001;8:557.
- [10] Y. Suzuki, T. Miyanaga, H. Hoshino, N. Matsumoto, T. Aina. In-situ XAFS study of Ag clusters in zeolite 4A. *Phys Scr.* 2005;T115:765.
- [11] H. Hoshino, Y. Sannohe, Y. Suzuki, T. Azuhata, T. Miyanaga, K. Yaginuma, M. Itoh, T. Shigeno, Y. Osawa, Y. Kimura. Photoluminescence of the dehydrated Ag-type zeolite A packed under air. *J. Phys. Soc. Jpn.* 2008;77(6):064712.
- [12] A. Nakamura, M. Narita, S. Narita, Y. Suzuki, T. Miyanaga. In-situ XAFS study of Ag clusters in Ag-type zeolite-A. *J. Phys. Conf. Ser.* 2014;502:012033.
- [13] H. Sakane, T. Miyanaga, I. Watanabe, N. Matsubayashi, S. Ikeda, Y. Yokoyama. Reproducibility tests of extended X-ray absorption fine structure for aqua and amine complexes of first transition metals in solid and aqueous solution. *Jpn. J. Appl. Phys.* 1993;32:4641.
- [14] Available from: <http://cars.uchicago.edu/ifeffit/Downloads> 2016.5.21
- [15] A.L. Ankudinov, B. Ravel, J.J. Rehr, S.D. Conradson. Real space multiple scattering calculation of XANES. *Phys. Rev. B.* 1998;58:7565.
- [16] S.A. Rodrigues. Vibrational spectroscopy and structural analysis of Na–Y zeolite. *Vib. Spectrosc.* 1995;9:225.